Molecular Biology of the Cell
Vol. 18, 1272–1281, April 2007

Junction Protein Shrew-1 Influences Cell Invasion and Interacts with Invasion-promoting Protein CD147

Alexander Schreiner,* Mika Ruonala,† Viktor Jakob,* Jan Suthaus,‡ Eckhard Boles,§ Fred Wouters,† and Anna Starzinski-Powitz*

*Institute of Cell Biology and Neuroscience, Johann Wolfgang Goethe University of Frankfurt, D-60323 Frankfurt am Main, Germany; †European Neuroscience Institute Göttingen, D-37077 Göttingen, Germany; ‡Institute of Biochemistry, Christian-Albrechts-Universität Kiel, D-24098 Kiel, Germany; and §Institute of Molecular Biosciences, Johann Wolfgang Goethe University of Frankfurt, D-60438 Frankfurt am Main, Germany

Submitted July 27, 2006; Revised December 6, 2006; Accepted January 22, 2007
Monitoring Editor: Asma Nusrat

Shrew-1 was previously isolated from an endometriotic cell line in our search for invasion-associated genes. It proved to be a membrane protein that targets to the basolateral membrane of polarized epithelial cells, interacting with E-cadherin–catenin complexes of adherens junctions. Paradoxically, the existence of adherens junctions is incompatible with invasion. To investigate whether shrew-1 can indeed influence cellular invasion, we overexpressed it in HT1080 fibrosarcoma cells. This resulted in enhanced invasiveness, accompanied by an increased matrix metalloprotease (MMP)-9 level in the supernatant, raising the question about the role of shrew-1 in this process. Logic suggested we looked for an interaction with CD147, a known promoter of invasiveness and MMP activity. Indeed, genetics-based, biochemical, and microscopy experiments revealed shrew-1– and CD147-containing complexes in invasive endometriotic cells and an interaction in epithelial cells, which was stronger in MCF7 tumor cells, but weaker in Madin-Darby canine kidney cells. In contrast to the effect mediated by overexpression, small interfering RNA-mediated down-regulation of either shrew-1 or CD147 in HeLa cells decreased invasiveness without affecting the proliferation behavior of HeLa cells, but the knockdown cells displayed decreased motility. Altogether, our results imply that shrew-1 has a function in the regulation of cellular invasion, which may involve its interaction with CD147.

INTRODUCTION

Invasion and metastasis of cells into surrounding tissue and to more distant locations is one of the most menacing properties of cancer diseases. Numerous molecules are important for the development of invasion, one of which is E-cadherin. The loss of E-cadherin was shown to promote invasiveness of tumor cells and is commonly associated with the development of carcinomas (Cavallaro and Christofori, 2001). The loss of E-cadherin–mediated cell-cell adhesion is also associated with an increased proteolytic activity of matrix metalloproteases (MMPs) (Curran and Murray, 1999). The regulation of MMPs is mediated by various mechanisms, for example, by direct cell–cell interactions (tumor–stroma or tumor cell–tumor cell interactions). In this context, the most prominent molecule is CD147, also known as extracellular matrix metalloprotease inducer (EMMPRIN) (Ellis *et al*., 1989; Kataoka *et al*., 1993; Sun and Hemler, 2001). CD147 is a multifunctional type 1 transmembrane protein with two extracellular Ig-like domains and a cytoplasmic domain of 40 amino acids, and it is typically targeted to the basolateral part of the plasma membrane in noninvasive epithelial cells (Biswas *et al*., 1995; Toole, 2003). Together with its MMP-inducing activity, CD147 is essential for correct plasma membrane targeting of monocarboxylate transporters MCT-1 and MCT-4, which remain perinuclear in the absence of CD147 (Kirk *et al*., 2000). Additionally, CD147 has a function as a receptor for cyclophilin A. Here, CD147 facilitates human immunodeficiency virus-1 infection by binding cyclophilin A, which is cotransported by the virus from its producer cell (Pushkarsky *et al*., 2001). In a recent publication, it was shown that CD147 is also a regulatory subunit of the gamma secretase complex and that it is involved in the regulation of amyloid β-peptide production (Zhou *et al*., 2005).

Endometriosis, defined as benign endometrium-like growth outside the uterine cavity, is one of the most frequently diagnosed gynecological diseases with an invasive phenotype (Cramer, 1987; Osteen *et al*., 1997). Moreover, endometriosis may be regarded as a paradigm for an invasive disease (Starzinski-Powitz *et al*., 2001). During the search for genes involved in invasion of endometriotic cells and possibly also in cancer, we identified shrew-1 (Bharti *et al*., 2004). Computer-based searches showed that the shrew-1 gene is located on chromosome 1p36.32 and that its protein sequence does not share any similarity with known proteins. Because shrew-1 homologues could only be found in zebrafish and mammals, it seems to be specific for vertebrates. Computational and experimental analyses have shown that shrew-1 is an integral membrane protein of 411 amino acids, the C terminus being intracellular (Bharti *et al*., 2004). In polarized epithelial cells shrew-1 is found at the basolateral part of the plasma membrane, where it colocalizes with, and apparently integrates into E-cadherin–mediated adherens

This article was published online ahead of print in *MBC in Press* (http://www.molbiolcell.org/cgi/doi/10.1091/mbc.E06–07–0637) on January 31, 2007.

Address correspondence to: Anna Starzinski-Powitz (starzinski-powitz@em.uni-frankfurt.de).

junctions. In vitro experiments suggest that this localization could be mediated by a direct interaction with β-catenin. In nonpolarized, highly migratory, and invasive epithelial cells, shrew-1 does not interact with cadherin–catenin complexes (Bharti *et al*., 2004). Finally, recent work has shown that the chromosomal locus 1p36, where shrew-1 is encoded, is frequently lost in oligodendrogliomas and neuroblastomas (Dong *et al*., 2004; White *et al*., 2005).

In this work, we combine small interfering RNA (siRNA) overexpression and imaging approaches to show the direct interaction of shrew-1 with the transmembrane glycoprotein CD147, a regulatory subunit of γ-secretase, an inducer of matrix metalloproteinase activity, and an essential component for cellular invasion. Our findings suggest that the shrew-1–CD147 interaction is associated with the regulation of cellular invasion. Shrew-1 may therefore be part of a regulatory network controlling cellular invasion.

MATERIALS AND METHODS

Antibodies

Mouse monoclonal anti-CD147 antibody (MEM-M6/1) was purchased from Immuno Tools (Friesoythe, Germany) (Western blot, 1 μg/ml; immunofluorescence, 10 μg/ml), mouse monoclonal anti-green fluorescent protein (GFP) was obtained from Roche Applied Science (Mannheim, Germany) (Western blot, 0.4 μg/ml) and mouse monoclonal anti-bromodeoxyuridine antibody (Bu20a) was from Dako Deutschland (Hamburg, Germany) (diluted 1:100). For detection of the birch profilin (BP) tag (S F P Q F K P Q E I), monoclonal antibody (mAb) 4A6 described previously (Rudiger *et al*., 1997) was used at a dilution of 1:1000. Polyclonal rat anti-shrew-1 antibodies were generated against the cytoplasmic domain of shrew-1 by Genovac (Freiburg, Germany). Secondary antibodies for immunofluorescence (AlexaFluor 488 goat anti-mouse IgG and AlexaFluor 594 goat anti-mouse IgG) were from Invitrogen (Karlsruhe, Germany) (5 μg/ml). The alkaline phosphatase-conjugated AffiniPure goat anti-mouse secondary antibodies for immunoblotting were from Jackson ImmunoResearch (Dianova, Hamburg, Germany) (0.12 μg/ml).

Cell Lines, Cell Culture, and Transfection

The endometriotic cell line 12z was established previously (Zeitvogel *et al*., 2001) and is similar to that from which shrew-1 was originally isolated. Further cell lines used were obtained from the American Type Culture Collection (Manassas, VA), HeLa (CCL-2), HT1080 (CCL-121), Madin-Darby canine kidney (MDCK) (CCL-34), or MCF7 (ECACC no. 86012803) from the European Collection of Cell Cultures (Salisbury, United Kingdom). Cells were cultured in Dulbecco's modified Eagle's medium (DMEM) supplemented with 10% fetal calf serum (FCS) (PAA Laboratories, Cölbe, Germany) and 1% penicillin/streptomycin in an atmosphere of 10% CO_2 and 95% humidity. DMEM and penicillin/streptomycin were purchased from Invitrogen. Transfections were performed using magnet-assisted transfection (MATra; IBA, Göttingen, Germany) as follows: cells were cultured in six-well plates, and upon 60% confluence, HeLa, HT1080, and MCF7 cells were transfected with a total of 1.5 μg of DNA, and MDCK cells with a total of 2 μg of DNA. A corresponding volume of MATRa reagent (1.5 μl for HeLa, HT1080, and MCF7, and 2 μl for MDCK cells) was mixed with serum-free DMEM and transferred to another tube containing the DNA. After thorough mixing, the DNA–MATRa complexes were allowed to form for 20 min at room temperature. After addition of the MATRa–DNA solution to the cells, the cell plates were placed on the MATRa magnet for 20 min in the cell incubator. Cells were then kept in the incubator for the desired time.

Flow Cytometry

The percentage of GFP and shrew-1–GFP-positive HT1080 cells was analyzed by flow cytometry by using a FACSAria cell sorting system (Becton Dickinson, Heidelberg, Germany). For each cell clone 3×10^4 events were analyzed. The data were further processed using Windows multiple documentation interfaces, flow cytometry application (WinMDI version 2.9).

Cloning of CD147 Yellow Fluorescent Protein (YFP) and Shrew-1 Cyan Fluorescent Protein (CFP)

To clone CD147, total RNA was prepared from MCF7 cells using the RNeasy Midi kit from QIAGEN (Hilden, Germany) according to the manufacturer's manual, except that the lysate was processed 15 times through the needle of a syringe. Then, 4 μg of RNA was transcribed into cDNA by using Moloney murine leukemia virus reverse transcriptase (Promega, Mannheim, Germany) according to the manufacturer's protocol. CD147 was cloned into pEYFP-N1 (Clontech, Saint-Germain-en-Laye, France) between EcoRI and BamHI restriction sites by using suitable oligonucleotides (sequence-specific nucleotides are underlined): CD147 fwd., 5′-CGGAATTCATGGCGGCTGCGCTGTTCG-3′ and CD147 rev., 5′-CGGGATCCAAGGAAGAGTTCCTCTGGCG-3′. Shrew-1-CFP was derived by amplifying the shrew-1 coding sequence from pEGFP shrew-1 and cloning this into pECFP-N1 (Clontech) by using EcoRI and Acc65I and the following oligonucleotides (sequence-specific nucleotides are underlined): shrew-1 fwd., 5′-GAATTCATGTGGATTCAACAGCTT-3′ and shrew-1 rev., 5′-GGTACCAAGCAGGAGATTTCAAACCATT-3′. Success of the cloning was verified by sequencing and expression analyzed by Western blotting.

siRNA Cloning and Stable Selection

To knockdown shrew-1 or CD147, different target sequences were cloned into psilencer 2.1 Hygro (Ambion, Austin, TX) according to the manufacturer's protocol and expressed as small hairpin RNAs. The target sequences were selected by analyzing the corresponding mRNA sequences with the target finder (available online from Ambion). The following oligonucleotide sequences were chosen and ordered from MWG-Biotech (Ebersberg, Germany) (target sequences are underlined): shrew-1 sequence A fwd., 5′-GATCCGCACATTTCCGGGCGTTTACTTCAAGAGAGTAAACGCCCGGAAATGTGTTTTTTGGAAA-3′ and shrew-1 sequence A rev., 5′-AGCTTTTCCAAAAAACACATTTCCGGGCGTTTACTCTCTTGAAGTAAACGCCCGGAAATGTGCG-3′; shrew-1 sequence B fwd., 5′-GATCCGCGAGACCCTGCAGTGTTCTTTCAAGAGAAGAACACTGCAGGGTCTCGTTTTTTGGAAA-3′ and shrew-1 sequence B rev., 5′-AGCTTTTCCAAAAAACGAGACCCTGCAGTGTTCTTCTCTTGAAAGAACACTGCAGGGTCTCGCG-3′; CD147 fwd., 5′-GATCCGACCTTGGCTCCAAGATACTTCAAGAGAGTATCTTGGAGCCAAGGTCTTTTTTGGAAA-3′ and CD147 rev., 5′-AGCTTTTCCAAAAAAGACCTTGGCTCCAAGATACTCTCTTGAAGTATCTTGGAGCCAAGGTCG-3′; and negative control fwd., 5′-GATCCGGTTATGTACAGGAACGCATTCAAGAGATGCGTTCCTGTACATAACCTTTTTTGGAAA-3 and negative control rev., 5′-AGCTTTTCCAAAAAAGGTTATGTACAGGAACGCATCTCTTGAATGCGTTCCTGTACATAACCG-3′. Cells were selected with 166 μg/ml hygromycin beginning 24 h after transfection.

Split Ubiquitin Interaction Assay

The split ubiquitin system used was described previously (Obrdlik *et al*., 2004). The following oligonucleotides were used to amplify shrew-1 coding sequence; linker sequences needed for homologous recombination are underlined: shrew-1 fwd., 5′-ACAAGTTTGTACAAAAAAGCAGGCTCTCCAACCACCATGTGGATTCAACAGCTTTTA-3′ and shrew-1 rev., 5′-TCCGCCACCACCAACCACTTTGTACAAGAAAGCTGGGTAGCAGGAGATTTCAAACCATTT-3′. Cloning of CD147 and MCT-1 was described previously (Makuc *et al*., 2004). The following few changes were made, after selection of single transformants, colony polymerase chain reactions (PCRs) were performed using the same oligonucleotides as for cloning. Single positive colonies were then mated and further processed as described, but the final selection plates were incubated for 3–5 d. To verify the growth of yeast cells on final selection plates, some colonies were replated onto final selection plates and subjected to a β-galactosidase filter lift assay. The filter assay was performed according to the two-hybrid instruction manual of Stratagene (Heidelberg, Germany) to ensure that yeast growing on final selection plates was not due to leaky expression of the *HIS3* gene or to residual amino acids from mating plates, but to a true interaction.

Coimmunoprecipitation

Cells were grown to confluence, washed twice with ice-cold phosphate-buffered saline (PBS), and lysed for 20 min at 4°C in a buffer containing 10 mM Tris, pH 8.0, 150 mM NaCl, 5 mM EDTA, 1% Triton X-100, and 60 mM *n*-octyl-glucoside. We kept 10% of the lysis volume as input control; the rest of the sample was precleared for 1 h at 4°C with protein G-Sepharose (30 μl; 1:1 in lysis buffer) and subjected to immunoprecipitation overnight at 4°C by using a rat polyclonal shrew-1 antibody (original serum was diluted 1:20). Immunocomplexes were precipitated by incubation with 30 μl of protein G-Sepharose (1:1 in lysis buffer) for 2 h at 4°C. After four washes with the lysis buffer, samples were separated by SDS-PAGE. The coimmunoprecipitation of CD147 was performed under nonreducing conditions. Afterward, the separated samples were transferred to a nitrocellulose membrane and probed with appropriate antibodies.

Immunoblotting

Cells were grown in 10-cm dishes to confluence, washed with PBS, and lysed with 300 μl of radioimmunoprecipitation assay buffer (150 mM NaCl, 50 mM Tris-HCl, pH 7.5, 0.25% sodium deoxycholate, 0.1% Nonidet P-40, and 0.1% SDS) plus proteinase inhibitor cocktail Complete (Roche Applied Science) for 10 min at 4°C. Lysates were cleared by centrifugation for 5 min at 4°C in a microcentrifuge. From the cleared extract, 20 μg of total protein was separated by SDS-PAGE and transferred onto nitrocellulose membranes in a semidry blotting chamber (PEQLAB Biotechnologie, Erlangen, Germany). A prestained protein standard was used as a molecular size marker (SDS7B protein ladder, Sigma-Aldrich Chemie, München, Germany). Membranes

were blocked with 4% nonfat milk powder in Tris-buffered saline/Tween (10 mmol/l Tris-HCl, pH 7.4, 150 mmol/l NaCl, and 0.1% Tween 20) for 1 h. After a single wash step with TBST, the membranes were incubated with primary antibody for 2 h at room temperature, and after intensive washing, the bound primary antibody was detected with alkaline phosphatase conjugated secondary antibody (Dianova). Nitro blue tetrazolium and 5-bromo-4-chloro-3-indolyl phosphate (Roche Applied Science) were used as the substrates.

Immunofluorescence, Confocal Microscopy, and Förster Resonance Energy Transfer (FRET) Analysis

Cells were grown on glass coverslips, and upon reaching the desired confluence, they were fixed for 30 min with 4% paraformaldehyde (in PBS), washed two times for 5 min with PBS, and permeabilized for 5 min with 0.1% Triton X-100 (in PBS). Then, they were incubated for 10 min in 50 mM glycine (in PBS). In FRET analysis, cells were then washed again two times for 5 min with PBS, and afterward they were mounted using Mowiol (Mowiol 4-888; Sigma-Aldrich Chemie) without anti-fading reagent.

For immunofluorescent labeling, the cells were blocked for 30 min with 10% FCS/PBS. Primary antibodies were diluted in 10% FCS/PBS and incubated either for 2 h at room temperature or overnight at 4°C. Antibody binding was visualized by fluorochrome-conjugated secondary antibodies. Nuclei were stained with Hoechst dye no. 33258 (Sigma-Aldrich Chemie). The samples were examined either with an Axiophot (Carl Zeiss, Göttingen, Germany) or a TCS NT confocal laser scanner microscope (Leica Microsystems, Heidelberg, Germany). Images were processed with Image ProPlus (Media Cybernetics, Silver Spring, MD) and Imaris (Bitplane, Zürich, Switzerland) and prepared for publication with Adobe Photoshop (Adobe Systems, Unterschleissheim, Germany).

For FRET analyses, the CFP in cells expressing either shrew-1-CFP alone, or with CD147-eYFP, was excited with a Mira 900 two-photon laser tuned to 820-nm excitation wavelength. The fluorescence lifetime (τ) of CFP was determined by a time correlated single photon counting (TCSPC; Beckel & Hickl, Berlin, Germany) module coupled to a TCS SP2 AOBS confocal microscope (Leica Microsystems) in a pixel-by-pixel manner. The fluorescence lifetime was analyzed using SPCImage software (Beckel & Hickl) with binning and background thresholding to obtain optimum photon count and signal-to-noise ratio for reliable statistical analysis. The images were further analyzed using ImageJ software (W. Rasband, National Institutes of Health, Bethesda, MD). A chi square filter of 2.5 was applied on the τ images, and the τ distribution histograms from several measured cells were summarized and normalized against the number of available pixels. The cumulative FRET efficiencies of the samples' histograms were plotted using the donor-only histogram as the baseline (FRET efficiency = 0%).

Matrigel Invasion Assays and Gelatin Zymography

The invasiveness of cells was analyzed using Falcon BioCoat Matrigel chambers (Becton Dickinson) with 6.4-mm diameter and 8-μm pore size. Invasiveness of HT1080 cells was assayed as described previously (Zeitvogel *et al*., 2001), and the analysis on HeLa cells was performed according to Saito *et al*. (1997). Briefly, 5×10^4 HeLa cells were seeded on the upper side of a Matrigel invasion chamber. After 48 h, the cells were fixed with methanol and stained with crystal violet. Incorporated dye was extracted with acetic acid, and the amount measured by absorption at 590 nm. Two filters were used for a single experiment and cell clone: one filter was analyzed on the upper side (noninvasive cells), and the other filter on the lower side (invasive cells). The absorption readings from the upper and lower side were added to yield the total absorption, and invasiveness was calculated as a percentage of the lower side absorption over the total absorption. The statistical significance was estimated with a student's *t* test for unpaired samples.

Gelatin zymography was used to analyze proteolytic activity in the supernatant of cultured cells. Cells were cultured for 24 h in medium containing no FCS, and then the supernatant was collected and centrifuged for 2 min at 12,000 $\times$ *g*. In addition, the cells were lysed, and the protein concentration was determined. The volume of supernatant collected was normalized to the protein concentration to ensure equal loading. The supernatants were separated in SDS gels containing 1 mg/ml gelatin in the resolving gel. The loading buffer did not contain reducing agents (0.2 M Tris-HCl, pH 6.8, 40% glycerol, 8% SDS, and 0.01% bromphenol blue solution). After running the gel, it was

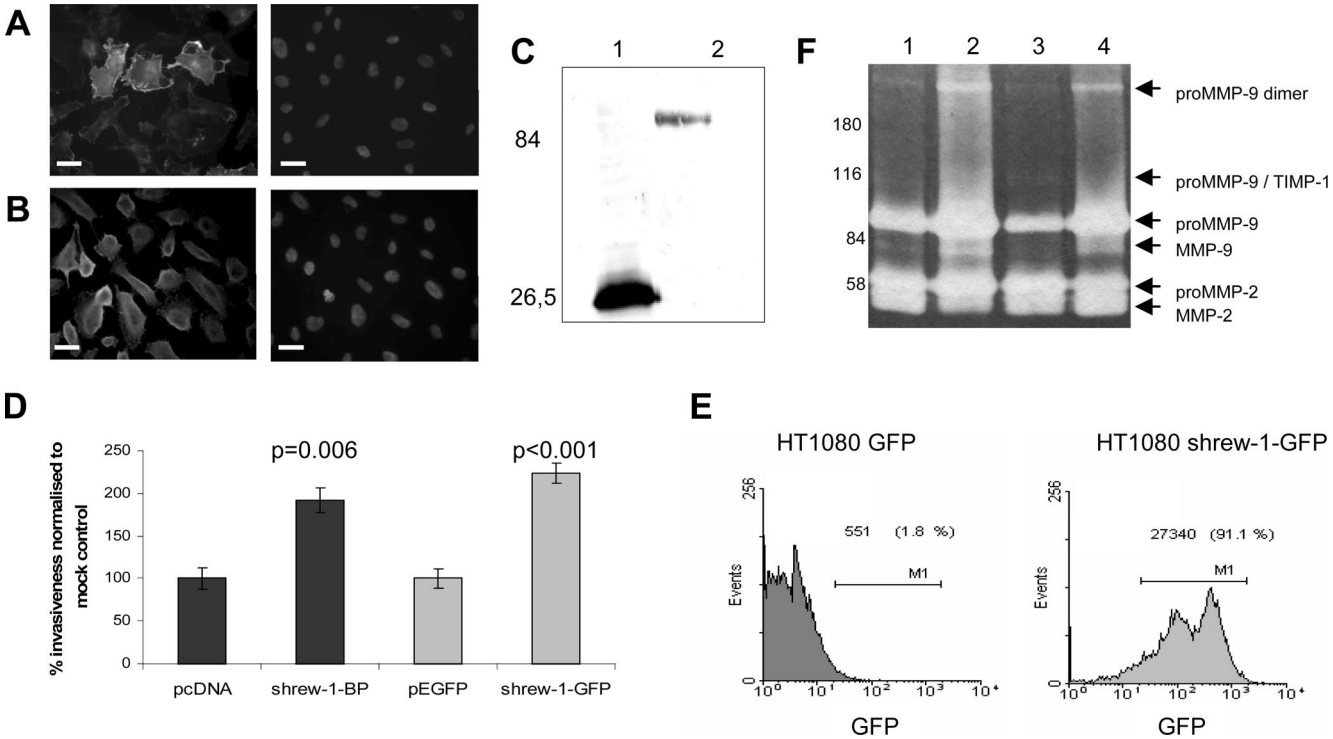

Figure 1. Overexpression of shrew-1 enhances invasiveness. HT1080 cells were stably transfected with shrew-1-GFP or shrew-1-BP. (A and B) Positive expression was shown for shrew-1-GFP by fluorescence microscopy (A) and for shrew-1-BP by immunofluorescence microscopy (B). Right, 4′,6-diamidino-2-phenylindole (DAPI)-stained nuclei. (C) Shrew-1-GFP expression was also shown by immunoblotting of whole cell extracts by using an anti-GFP antibody (1, pEGFP vector control; 2, shrew-1-GFP). Numbers on the left indicate molecular mass in kilodaltons. (D) Impact on invasiveness was analyzed by Matrigel invasion assays. Compared with the vector controls (pcDNA and pEGFP), shrew-1–overexpressing cells showed a significant increase in invasiveness. Error bars indicate SE of the mean; p values were calculated by a Student's *t* test (http://www.physics.csbsju.edu/stats/t-test.html) (n = 3). (E) About 90% of the cells express shrew-1-GFP as analyzed by flow cytometry. (F) The supernatants of shrew-1-BP– (2) and shrew-1-GFP (4)–overexpressing cells as well as the corresponding vector controls (1, pcDNA; 3, pEGFP) were analyzed by gelatin zymography. Numbers on the left indicate molecular mass in kilodaltons. Bar, 20 μm.

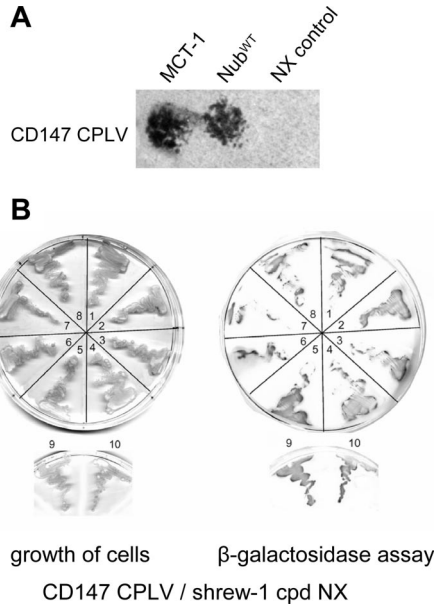

Figure 2. Split ubiquitin analysis of shrew-1 CPD interaction with full-length CD147 in yeast. Shrew-1 CPD sequence was amplified by PCR and cloned into split ubiquitin vectors by homologous recombination. After mating, final selection plates were incubated for 4 d at 30°C (A and B). (A) CD147 and MCT-1 positively interacted, whereas no growth was observed after mating CD147-expressing yeast strains with those transfected with empty NX vector (NX control). (B) CD147 interaction with shrew-1 CPD NX was tested. The plates showing growth after mating shrew-1 CPD NX with CD147 CPLV were subjected to a β-galactosidase filter lift assay (B, right) to verify the interaction. All clones were positive for β-galactosidase activity, indicating a positive interaction between shrew-1 CPD and CD147. CD147 CPLV, full-length CD147 as a CPLV fusion; MCT-1, monocarboxylate transporter-1 NX fusion; Nub^{wt}, soluble wild-type Nub (N-terminal ubiquitin half); NX control, empty NX vector; and shrew-1 CPD NX, cytoplasmic domain of shrew-1 as NX fusion.

incubated in a renaturing buffer (2.5% Triton X-100 in H_2O) for 30 min and then preincubated in developing buffer (50 mM Tris-HCl, pH 7.6, 0.2 M NaCl, 5 mM $CaCl_2$, and 0.02% Brij 35) for 30 min at room temperature. The developing buffer was then renewed and incubated overnight at 37°C. For analysis, the gel was stained with Coomassie brilliant blue and partially destained.

Wound Healing Assay

For the analysis of HeLa cell migratory behavior, 3×10^5 cells were seeded in six-well plates and after forming a confluent monolayer, wounds were created using a 200-μl pipette tip. Two parallel wounds were created in each six-well, and their location was marked on the bottom of the six-well plate; 12 wounds were created for each cell clone. Images were taken after 6, 12, 18, 24, 36, and 42 h. Wound closure of control cells after 24 h was set to 100% and used as a reference for shrew-1 and CD147 knockdown cells.

5-Bromo-2′-deoxyuridine (BrdU) Labeling

BrdU labeling was performed to compare the proliferation rate of the cell clones. Cells were synchronized by a double thymidine block (Stein *et al.*, 1998), grown on glass coverslips and then fixed with methanol for 6 or 24 h after BrdU addition. BrdU incorporation was visualized using anti-BrdU antibody. Microscope images of BrdU and Hoechst staining were used to determine the percentage of BrdU-positive cells by counting three independent fields.

RESULTS

Overexpression of Shrew-1 Enhances Invasiveness

The isolation of shrew-1 from invasive cells raised the question of whether shrew-1 expression in such cells is directly involved in the regulation of invasion. To address this issue, we first overexpressed shrew-1 as either a GFP fusion protein or a BP-tagged protein in HT1080 cells. The expression of shrew-1-GFP was verified by fluorescence microscopy and Western blotting (Figure 1, A and C), and expression of shrew-1-BP was verified by immunofluorescence microscopy (detected with mAb 4A6) (Figure 1B). Analysis of shrew-1-GFP expression by flow cytometry revealed that 91% of the cells expressed shrew-1-GFP (Figure 1E). Matrigel invasion assays were performed to test whether shrew-1 overexpression had an effect on invasiveness, and indeed, HT1080 cells stably expressing either shrew-1-GFP or shrew-1-BP showed significantly higher invasiveness compared with control cells (Figure 1D). A prerequisite for cell invasiveness in this type of assay is sufficient expression of MMPs to degrade the Matrigel plugging the filter pores. To confirm that increased invasiveness is accompanied by an increase in proteolytic activity, the supernatants were analyzed by gelatin zymography. The results showed that HT1080 cells express MMP-2 and MMP-9 and that overexpression of shrew-1 led to an increased level of proMMP-9/MMP-9, but MMP-2 levels seemed unaltered (Figure 1F). Thus, shrew-1 might be involved in the regulation of proMMP-9/MMP-9 in HT1080 cells.

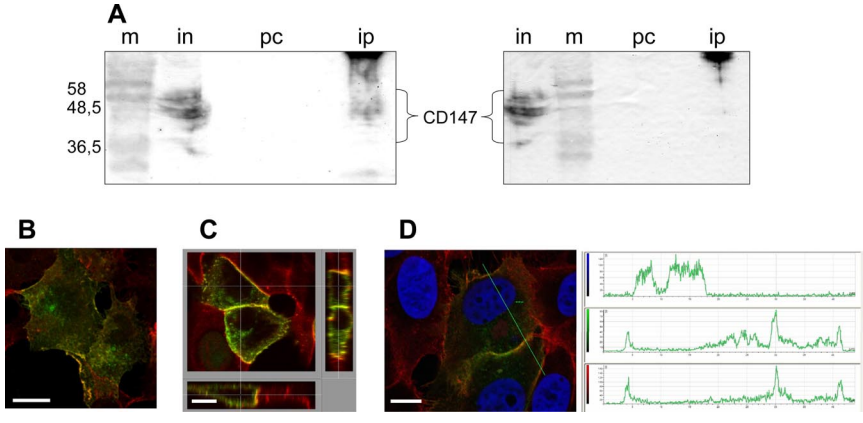

Figure 3. Shrew-1-GFP and CD147 coimmunoprecipitate from 12z cells and colocalize in HT1080 and MCF7 cells. (A) Left, coimmunoprecipitation of shrew-1 and CD147 from endometriotic cell line 12z (see *Materials and Methods*) by using an anti-shrew-1 antibody for precipitation is revealed by detecting CD147 in the ip by using anti-CD147 and immunoblotting. Numbers on the left indicate molecular mass in kilodaltons. (A) Right, an unspecific antibody for precipitation and anti-CD147 antibody for immunoblotting resulted in no co-ip. M, marker; in, input control; pc, preclearing. (B–D) HT1080 (B) and MCF7 (C and D) cells were transfected with shrew-1 GFP (green) and endogenous CD147 was stained with antibody (red). Colocalization was visualized using confocal laser scanning microscopy and image processing with Imaris 4.0.4 (B and C) or Leica LCS Lite 2.5 (C). Both molecules colocalize at the plasma membrane, and in MCF7 cells, predominantly at the lateral part, as can bee seen in xz and yz axes (C). That the fluorescence maxima of shrew-1 GFP and CD147 are found at the same distance along the axis (green line) drawn over the cells (D) also indicates that the two molecules colocalize. Bar, 10 μm.

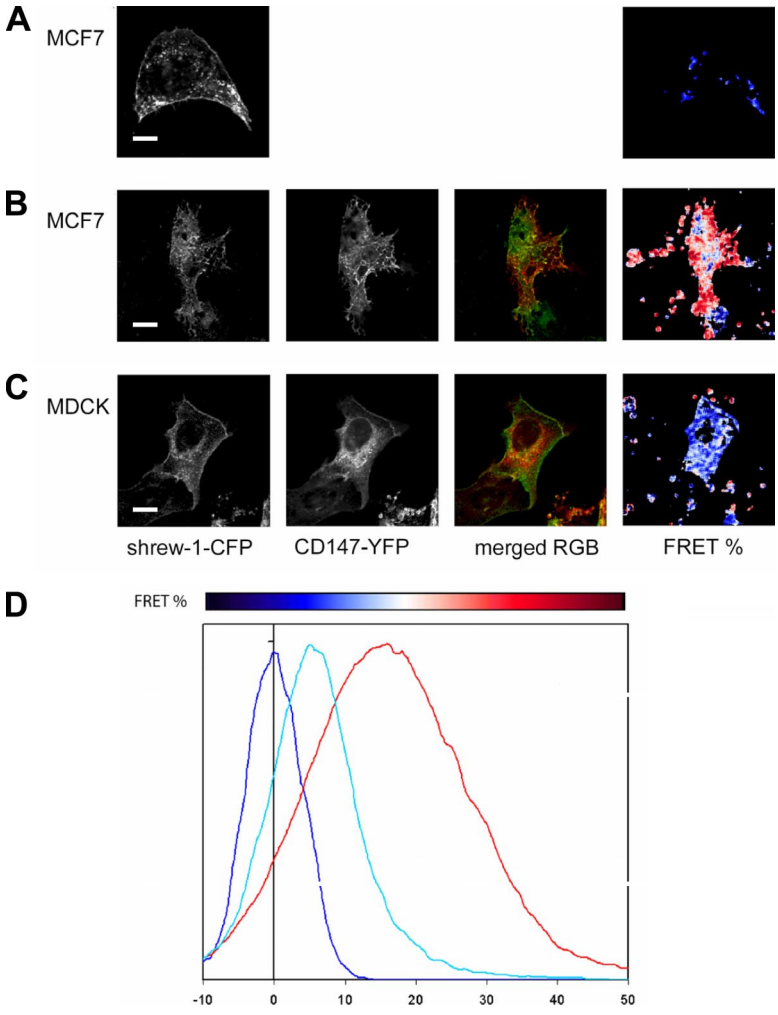

Figure 4. Interaction between shrew-1 and CD147 shown by FRET/FLIM. (A–D) MCF7 and MDCK cells were transfected with shrew-1-CFP and CD147-YFP either alone or together. A high FRET percentage means a significant decrease in the fluorescence lifetime of the donor, and this in turn indicates a close interaction. (A) The fluorescence lifetime of the donor (shrew-1-CFP) was determined from cells transfected with only this vector. (B) The decrease of lifetime in cotransfected MCF7 cells, shown by high FRET%, indicates a close interaction of shrew-1 and CD147. (C) MDCK cells in contrast show only a little FRET%. (D) In the graphical view, the lifetime of the donor alone (dark blue) is set to 0% FRET. MDCK cells (light blue) show only low FRET%, whereas MCF7 cells (red) show prominent FRET%. Bar, 10 μm.

Shrew-1 Interacts with CD147 in the Yeast Split Ubiquitin System

We next looked for a potential interaction partner that would help explain shrew-1's positive effect on invasiveness and the proteolytic activity in the supernatant of HT1080 cells (Figure 1C). As an educated guess, we chose CD147, because it is known to modulate the proteolytic activity of MMPs. We used a yeast-based split ubiquitin method to test for a potential interaction between shrew-1 and CD147. Here, the cytoplasmic domain of human shrew-1 (shrew-1 CPD) was expressed as a fusion protein with its N terminus fused to the N terminus of ubiquitin (NX). CD147 (full length) was expressed as a fusion with the C terminus of ubiquitin fused to a cleavable reporter (XCPLV).

As a positive control for the expression of CD147, recently reported to be functionally expressed in yeast (Makuc *et al.*, 2004), we used the known interaction between CD147 and MCT-1, as already shown in mammalian cells by FRET analysis (Wilson *et al.*, 2002). An additional positive control for reporter cleavage was expression of the wild-type form of the N-terminal ubiquitin half (Nub^{wt}), which leads to constitutive cleavage of the reporter. Growth upon mating yeast cells expressing Nub^{wt} and XCPLV fusion protein signifies a CPLV protein conformation that permits reconstitution of functional ubiquitin.

As expected, the control CD147–MCT-1 interaction resulted in yeast growth, whereas no growth was observed after mating CD147-positive yeast with yeast expressing the empty NX vector (Figure 2A). The cytoplasmic domain of shrew-1 expressed as a NX fusion protein also interacted with CD147 expressed as the XCPLV fusion (Figure 2B). To verify that the shrew-1 and CD147 interaction is specific and that the growth is not due to residual amino acids from mating plates, the clones were subjected to a β-galactosidase assay. All of the clones were positive for β-galactosidase (Figure 2B) as shown by a filter lift assay using 5-bromo-4-chloro-3-indolyl-β-D-galactoside as a substrate. This strongly supports a direct interaction between shrew-1 and CD147.

Coimmunoprecipitation and Colocalization of Shrew-1 and CD147

To show that shrew-1 and CD147 are present in the same complex, we performed coimmunoprecipitation assays with a polyclonal anti-shrew-1 antibody that pulls down endogenous shrew-1 from an endometriotic cell line (12z) (Zeitvogel *et al.*, 2001). The 12z cell line is equivalent to the cell line from which shrew-1 was originally isolated (Bharti *et al.*, 2004). CD147 was visualized in subsequent Western blots by using an antibody that detects all glycosylated forms of CD147 under nonreducing conditions. As shown in Figure 3A, left, CD147 coimmunoprecipitates (ip) with shrew-1. It should be noted that the reverse approach, using the anti-CD147 antibody for precipitation, was not feasible, because the anti-shrew-1 polyclonal antibody does not function in Western

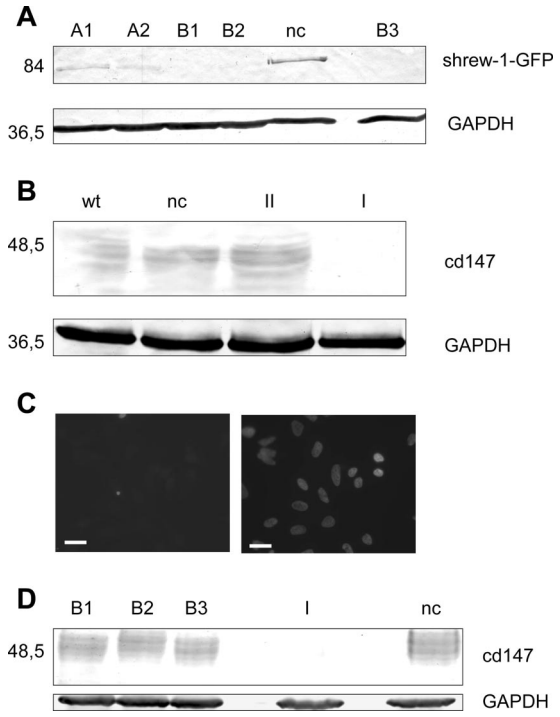

Figure 5. Down-regulation of shrew-1 and CD147 by RNA interference. HeLa cells were stably transfected with psilencer constructs producing shrew-1 A, shrew-1 B, cd147, and nc siRNAs. (A) Down-regulation of shrew-1 was analyzed by transfecting stable cell clones with shrew-1 GFP and separating 20 μg of whole cell lysates by 10% SDS-PAGE followed by immunoblotting by using an anti-GFP antibody. HeLa cells stably transfected with nc siRNA served as a control. Two clones stably transfected with psilencer shrew-1 A (A1 and A2) both showed detectable shrew-1 GFP expression, although visibly decreased compared with psilencer nc cells. In contrast, all HeLa cell clones stably transfected with psilencer shrew-1 B (B1–B3) showed no detectable expression of shrew-1 GFP. Numbers on the left indicate molecular mass in kilodaltons. (B) Down-regulation of CD147 was analyzed by separating 30 μg of whole cell lysate by 10% SDS-PAGE and simple immunoblotting by using an anti-CD147 antibody. Untransfected HeLa cells (wt) and HeLa cells stably transfected with psilencer nc both express CD147. From two clones stably transfected with psilencer CD147 (I and II), only clone I showed effective knockdown of CD147. Numbers on the left indicate molecular mass in kilodaltons. (C) Immunofluorescence analysis of CD147 knockdown cells with an anti-CD147 antibody confirms the almost complete absence of CD147. Right, DAPI-stained nuclei. Bar, 15 μm. (D) No alterations in the level of CD147 expression is detectable in shrew-1 knockdown cells (B1–B3), and no expression is detected in the CD147 knockdown clone (I) as shown by separating 30 μg of whole cell lysate by 10% SDS-PAGE and immunoblotting by using an anti-CD147 antibody. Numbers on the left indicate molecular mass in kilodaltons. To ensure loading of equal amounts of protein the blots were reprobed with anti-glyceraldehyde-3-phosphate dehydrogenase (GAPDH) (A, B, and D, bottom).

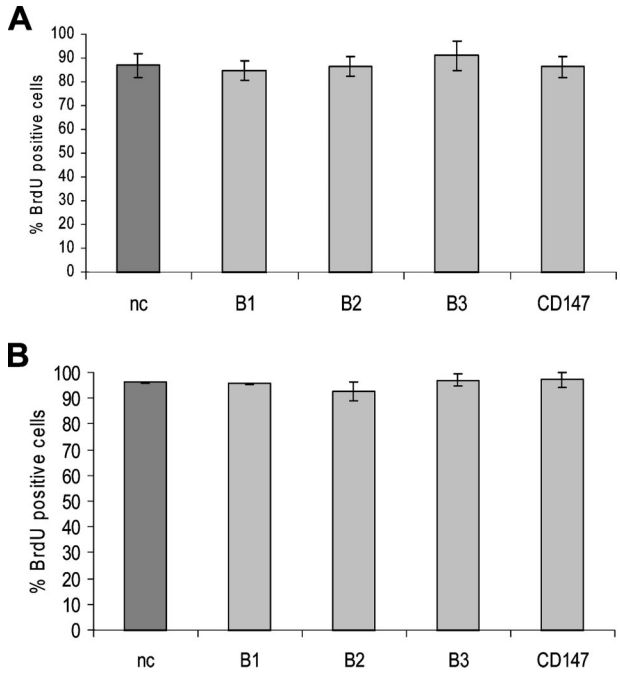

Figure 6. Proliferation of knockdown cells is comparable with control cells. Synchronized HeLa cells stably transfected with psilencer nc, psilencer shrew-1 B (B1–B3), or psilencer CD147 were labeled with BrdU for 6 (A) or 24 (B) h. Cells were then analyzed for incorporation of BrdU (i.e., proliferation) by immunofluorescence microscopy by using an anti-BrdU antibody. The bar graphs represent the percentages of BrdU-positive cells compared with DAPI-stained nuclei. No significant differences in BrdU incorporation at either time point were detectable. Error bars indicate the SD (n = 3).

blots. Control coimmunoprecipitation by using an unspecific antibody for precipitation and an anti-CD147 antibody for Western blotting led to no detectable coimmunoprecipitation of CD147 (Figure 3A, right), verifying the specificity of the shrew-1/CD147 coimmunoprecipitation, and, of course, the expression of both shrew-1 and CD147 in endometriotic cells.

The observation that shrew-1 and CD147 can form a complex was further supported by experiments showing that shrew-1-GFP colocalizes with endogenous CD147 in HT1080 cells (Figure 3B). Together, the coimmunoprecipitation in invasive endometriotic cells and the colocalization data in HT1080 cells strongly suggest that shrew-1 and CD147 are present in the same protein complex. This is supported by the direct interaction between shrew-1 and CD147 in biomolecular fluorescence complementation assays in HT1080 cells (data not shown).

Interestingly, shrew-1 and CD147 are also known to localize at the basolateral membrane of noninvasive epithelial cells (Bharti *et al.*, 2004; Deora *et al.*, 2004). Therefore, if the two proteins interact, they may also colocalize at the basolateral part of the plasma membrane. To test this, we investigated the subcellular localization of shrew-1-GFP with endogenous CD147 in MCF7 cells, and we observed strong colocalization of shrew-1-GFP and endogenous CD147 on the plasma membranes of these cells. As expected, colocalization was most prominent in the lateral region (Figure 3C). If the fluorescence intensities of shrew-1 GFP and antibody-stained CD147 were followed along a cell axis, the fluorescence maxima of both molecules occurred at the same region, indicating colocalization, or at least localization in proximity (Figure 3D).

Interaction Shown by FRET–Fluorescence Lifetime Imaging Microscopy (FLIM)

To confirm the shrew-1–CD147 interaction seen in yeast (Figure 2B) and the complex formation shown by coimmunoprecipitation (Figure 3C) in mammalian epithelial cells, we used one more approach, namely, FRET. FRET was determined by FLIM. In FRET–FLIM, reduction in the characteristic fluorescence lifetime of the donor fluorochrome (e.g., CFP) indicates a direct interaction of the donor with a

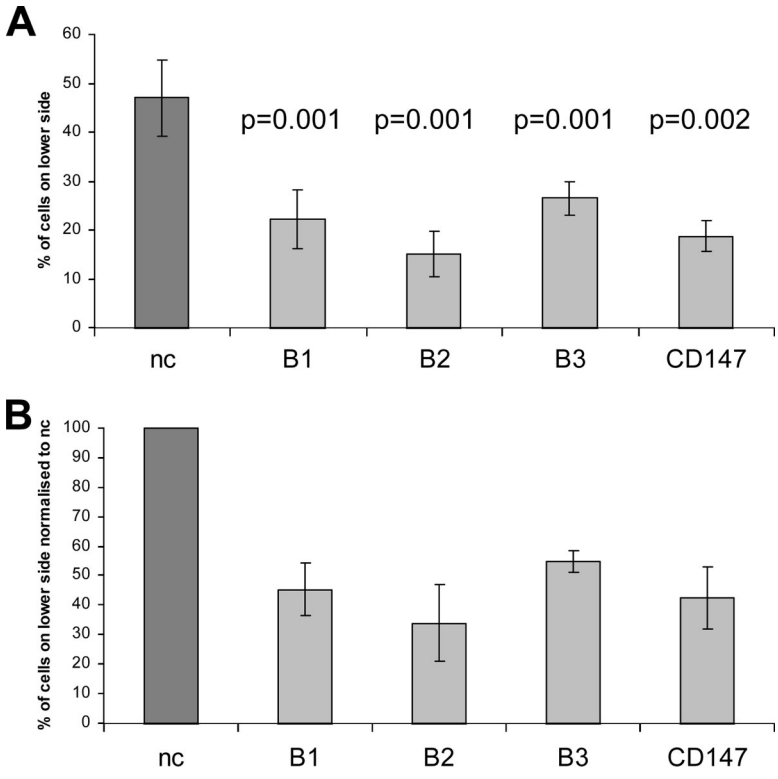

Figure 7. Matrigel invasion assay of shrew-1 and CD147 knockdown cells revealed a decrease in invasion compared with control cells. HeLa cells stably transfected with psilencer nc, psilencer shrew-1 B (clones B1–B3), or psilencer CD147 were tested in a matrigel invasion assay as described in *Materials and Methods*. Results from the lower side (invasive cells) compared with the total absorption value, i.e., the combined lower and upper (noninvasive) values, yield the percentage of cells that had reached the lower filter. (A) Knockdown of both shrew-1 and CD147 let to a significant reduction in invasiveness. (B) Normalization of the results to psilencer nc values showed a 35–55% decrease in invasiveness. Error bars indicate the SD, p values were calculated by a Student's *t* test (http://www.physics.csbsju.edu/stats/t-test.html) (n = 3).

spectrally suitable acceptor molecule (e.g., YFP) (Harpur *et al*., 2001). We therefore transfected either shrew-1-CFP (donor) alone or together with CD147-YFP (acceptor) into MCF7 and MDCK cells. Forty-eight hours posttransfection, the cells were prepared for FRET–FLIM assays, and the fluorescence lifetime of the shrew-1-CFP was determined using TCSPC. Comparing the cumulative histograms of the fluorescence lifetime distribution of several shrew-1-CFP–expressing cells to those obtained from cells cotransfected with shrew-1-CFP and CD147-YFP revealed a significant reduction in the CFP lifetime (Figure 4, A–D). The clear reduction in fluorescence lifetime points to a direct shrew-1-CFP–CD147 interaction. Interestingly, the reduced FRET efficiency in MDCK cells expressing shrew-1-CFP and CD147-YFP might reflect specific cell context-dependent modulations in the shrew-1 CD147 interaction (light blue in Figure 4D).

Invasiveness of Shrew-1 and CD147 Knockdown Cells

That shrew-1 and CD147 interact in noninvasive MCF7 epithelial tumor cells raised the question whether down-regulation of either of the two proteins would result in a reduction of invasiveness in invasive carcinoma cells. To address this issue, we chose a vector-based siRNA approach to express short hairpin RNAs to down-regulate shrew-1 and CD147 expression levels. After identifying siRNA sequences specific for shrew-1 or CD147 that were able to down-regulate expression of either protein, we generated HeLa cell clones stably expressing these siRNAs or a control sequence. The cell clones were then analyzed for expression of the corresponding protein. The level of shrew-1 could not be analyzed by a simple Western blot, because the available shrew-1 antibody, as mentioned above, does not detect it in Western blots. Moreover, its lower affinity would not exclude residual expression of shrew-1. We therefore transfected the potential shrew-1 knockdown cells with shrew-1-GFP and analyzed its expression by immunoblotting with an anti-GFP antibody. As shown in Figure 5A, shrew-1-GFP was absent in cell clones expressing siRNA B, whereas cells expressing siRNA A or the control sequence expressed detectable, although not equivalent levels of shrew-1-GFP. Down-regulation of exogenous shrew-1-GFP, which is strongly expressed by the cytomegalovirus promoter, implies that endogenous RNA is also affected, as long as the target sequence designed from a GenBank entry does not differ from the endogenous sequence. This was checked by amplifying the endogenous sequence by reverse transcription-PCR and subsequent DNA sequencing (data not shown). Because siRNA A did not down-regulate shrew-1 expression as strongly as the three independent clones derived from siRNA B transfection, only cell clones containing siRNA B were used for further down-regulation analyses. In the case of CD147, we were able to select a cell clone with no detectable CD147 expression, as tested by Western blotting and immunofluorescence with a CD147-specific antibody (Figure 5, B and C). It is worth mentioning that down-regulation of shrew-1 did not affect the expression level of CD147 as shown by Western blotting (Figure 5D).

To exclude any possible negative effects of protein knockdown on the rate of proliferation, we performed a proliferation assay. HeLa shrew-1 and CD147 knockdown cells as well as control cells were synchronized by a double thymidine block, incubated with BrdU for 6 or 24 h, and then analyzed for BrdU incorporation. No significant difference in BrdU labeling was observed between the knockdown and control cells, verifying similar proliferation potentials (Figure 6, A and B).

The effect of shrew-1 and CD147 knockdown on the invasive properties of HeLa cells was investigated by Matrigel invasion assays. A significant reduction in invasiveness was observed in shrew-1 knockdown cells compared with the control cells (Figure 7A). Approximately 50% of the control

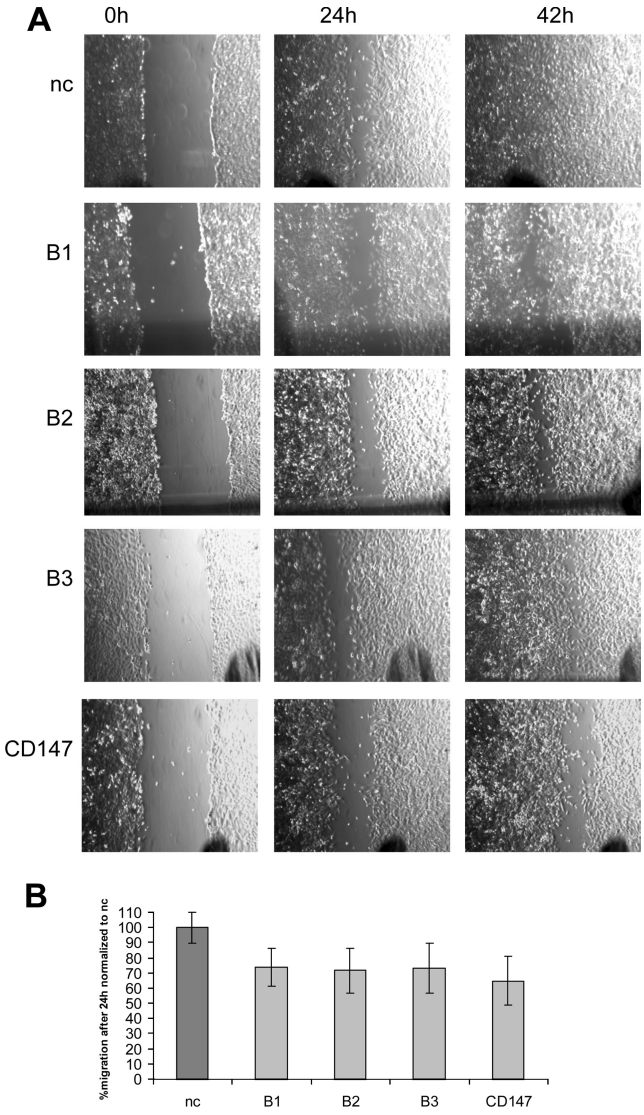

Figure 8. Knockdown of shrew-1 and CD147 alter the migratory behavior. (A) Wound healing assays were performed to test the migratory behavior of shrew-1 and CD147 knockdown cells. Images taken at different times after applying the wound were evaluated and compared. Whereas the wound was closed after 42 h with control cells (nc), it was not fully closed in the knockdown cells (B1–B3, shrew-1 knockdown; CD147, CD147 knockdown). (B) Graphical presentation of wound healing analyses. Wound closure was further analyzed by determining the migration of control cells (nc) after 24 h and setting this value to 100%. The migratory behavior of the shrew-1 (B1–B3) and CD147 knockdown cells was compared with that of control cells. Twelve different wounds were analyzed for each cell clone.

cells expressing the negative control (nc) siRNA were invasive, whereas only 15–25% of shrew-1 knockdown cells showed invasion in this assay. When normalized against the negative control, the invasiveness of knockdown cells was reduced by 50% (Figure 7B). A comparable result was obtained in HeLa cells expressing CD147 siRNA (Figure 7, A and B). This supports the idea that a shrew-1–CD147 interaction might be connected with the HeLa cells' invasive phenotype. Analyses of the proteolytic activity in the supernatant revealed no differences between knockdown and control cells (data not shown).

To analyze a possible effect of either shrew-1 or CD147 knockdown on another important feature of invasive cells, namely, their migratory behavior, we analyzed this by wound healing assays. Knockdown of both shrew-1 and CD147 resulted in delayed wound closure. As shown in Figure 8A, the control cells closed the wound after 42 h, whereas a comparable wound was not fully closed by the shrew-1 and CD147 knockdown cells over the same period. To compare the differences in migratory behavior, images were printed at the same size, and wound closure determined after 24 h was compared with closure of the control cells, which was set to 100%. As can be seen in Figure 8B, motility of the knockdown cells decreased by 27–36%. This result supports the idea that shrew-1 influences the migration/invasion of cells.

DISCUSSION

Our siRNA and overexpression experiments suggest that integral membrane protein shrew-1 plays a role in the invasive ability of tumor cells in culture. This is in line with our previous findings showing that the invasive parental endometriotic cell line from which shrew-1 was isolated expresses its mRNA, whereas the derivative that had lost invasiveness did not contain any detectable shrew-1 mRNA (Bharti *et al*., 2004). Identification of transmembrane protein CD147/EMMPRIN, a known promoter of cell invasion (Sun and Hemler, 2001), as a direct interaction partner of shrew-1, suggests that shrew-1's involvement in invasion is mediated through its interaction with CD147.

Interestingly, CD147 has been implicated in a variety of important cellular functions, one function of which is its known capacity to induce MMPs, which fits with an invasion promoting activity (Kataoka *et al*., 1993; Kirk *et al*., 2000; Sameshima *et al*., 2000; Sun and Hemler, 2001; Kanekura *et al*., 2002). These findings clearly suggest that shrew-1 itself may also be involved in such functions, at least in part. That knockdown of both shrew-1 and CD147 in HeLa cells leads to a similar decrease in migratory behavior as well as of invasion supports the argument that their interaction has a functional impact on these processes.

At first glance, shrew-1's influence on cellular invasion seems linked to increasing levels of MMP-9 in HT1080 cells, although it did not affect MMP-2. In HeLa cells, however, the knockdown of shrew-1 did not alter their proteolytic activity (data not shown), but they still have significantly reduced invasiveness. Thus, it could be argued that there is another functional aspect of shrew-1 contributing to regulation of invasion besides the effect on MMPs.

Interestingly, in addition to being identified by our group in invasive endometriosis cells, shrew-1 was also found to be differentially expressed in HT1080 cells selected for invasiveness. Although not published, this gene product was entered in the National Center for Biotechnology Information GenBank as MOT8. This also supports the conclusion that shrew-1 is a component of invasion controlling machinery in cancer cells, although the mechanism of shrew-1's contribution to this activity needs further exploration.

Our data further imply that the mere presence of shrew-1 and CD147 and their interaction is not sufficient to influence the invasive ability of the cells. This activity may only arise in the "right" cellular context. The basis for this argument is twofold. First, shrew-1 and CD147 interact in epithelial cells, which are noninvasive. Apart from this, the interaction is very different in MDCK and MCF7 cell lines, although both are epithelial cells. Also, they both exhibit a rather polarized phenotype with basolateral membrane compartments to

which both shrew-1 and CD147 can target (Deora *et al*., 2004; Jakob *et al*., 2006). A major and obvious difference between the two cell lines is that MDCK cells are rather "normal" and MCF7 are breast carcinoma cells. Thus, the stronger interaction between shrew-1 and CD147 in MCF7 cells compared with MDCK cells might relate to the tumor background of MCF7 cells.

Taking a closer look at the subcellular localization of shrew-1 reveals it is prominently targeted to the basolateral part of the plasma membrane in polarized epithelial cells, whereas in invasive cells it seems to be localized more or less all over the plasma membrane (Bharti *et al*., 2004). In the context of altered migratory behavior, it is noteworthy that CD147 can associate with $\alpha 3\beta 1$ and $\alpha 6\beta 1$ integrins (Berditchevski *et al*., 1997). The basal localization of shrew-1 (Bharti *et al*., 2004) leaves open the possibility that it is associated with integrins such as CD147.

Based on the ideas discussed above, shrew-1's function in general might be even more complicated when looking at cells of the CNS, such as neuronal and glial cells and tumors derived from them. Here, it seems the loss of shrew-1 expression has opposite effects compared with epithelial cells. This suggestion is based on recent publications showing that shrew-1's genomic location (1p36) is frequently lost in oligodendrogliomas or neuroblastomas (Dong *et al*., 2004; White *et al*., 2005), which is not known for carcinomas. Tumor-specific deletion of shrew-1 gene-containing chromosomal region or silencing presumably by hypermethylation was not detected in surrounding healthy tissue (McDonald *et al*., 2006). This is somewhat unexpected, because these tumors are clearly capable of invading surrounding tissue. In the same publication it was additionally shown that re-expression of shrew-1 in glioma tumor cells (U251) decreased cellular motility. Thus, there seems to be a contradiction between shrew-1's influence on cell migration in cells of the nervous system and other cells.

Concordant with these findings (Dong *et al*., 2004; White *et al*., 2005; McDonald *et al*., 2006) are our Northern blot analyses, which showed that shrew-1 mRNA is abundantly expressed in the brain (data not shown). Thus, down-regulation of shrew-1 expression associated with oligodendrogliomas and neuroblastomas suggests that shrew-1 may act as a tumor suppressor gene. This would seem to contradict our findings obtained in epithelial and mesenchymal cells. However, whether shrew-1's absence is compensated by some other molecule in the invasion controlling machinery of oligodendrogliomas and neuroblastomas remain to be investigated as well as the interaction of shrew-1 with CD147 in normal brain cells. Alternatively, shrew-1 might play no direct role in invasion of oligodendrogliomas and neuroblastomas per se, but it might have a very different function in normal brain, which only overlaps with its role in epithelial cells.

In summary, our results point to a role for shrew-1 in cellular invasion, possibly through its interaction with CD147, and they suggest that shrew-1 is a multifunctional protein whose interactions and thus functions may depend on, or be modulated by, the cellular context.

ACKNOWLEDGMENTS

We thank Avril Arthur-Goettig for critical reading of the manuscript, Monika Kamprad for experimental support, and Dr. S. Liebe (Leica, Bensheim, Germany) for technical support. This work was supported by Deutsche Forschungsgemeinschaft through grant SFB 628, project B1/P7.

REFERENCES

Berditchevski, F., Chang, S., Bodorova, J., and Hemler, M. E. (1997). Generation of monoclonal antibodies to integrin-associated proteins. Evidence that alpha3beta1 complexes with EMMPRIN/basigin/OX47/M6. J. Biol. Chem. *272*, 29174–29180.

Bharti, S., Handrow-Metzmacher, H., Zickenheiner, S., Zeitvogel, A., Baumann, R., and Starzinski-Powitz, A. (2004). Novel membrane protein shrew-1 targets to cadherin-mediated junctions in polarized epithelial cells. Mol. Biol. Cell *15*, 397–406.

Biswas, C., Zhang, Y., DeCastro, R., Guo, H., Nakamura, T., Kataoka, H., and Nabeshima, K. (1995). The human tumor cell-derived collagenase stimulatory factor (renamed EMMPRIN) is a member of the immunoglobulin superfamily. Cancer Res. *55*, 434–439.

Cavallaro, U., and Christofori, G. (2001). Cell adhesion in tumor invasion and metastasis: loss of the glue is not enough. Biochim. Biophys. Acta *1552*, 39–45.

Cramer, D. W. (1987). Epidemiology of endometriosis in adolescents. In: Endometriosis, ed. E. A. Wilson, New York: Alan Liss, 5–8.

Curran, S., and Murray, G. I. (1999). Matrix metalloproteinases in tumour invasion and metastasis. J. Pathol. *189*, 300–308.

Deora, A. A., Gravotta, D., Kreitzer, G., Hu, J., Bok, D., and Rodriguez-Boulan, E. (2004). The basolateral targeting signal of CD147 (EMMPRIN) consists of a single leucine and is not recognized by retinal pigment epithelium. Mol. Biol. Cell *15*, 4148–4165.

Dong, Z., Pang, J. S., Ng, M. H., Poon, W. S., Zhou, L., and Ng, H. K. (2004). Identification of two contiguous minimally deleted regions on chromosome 1p36.31-p36.32 in oligodendroglial tumours. Br. J. Cancer *91*, 1105–1111.

Ellis, S. M., Nabeshima, K., and Biswas, C. (1989). Monoclonal antibody preparation and purification of a tumor cell collagenase-stimulatory factor. Cancer Res. *49*, 3385–3391.

Harpur, A. G., Wouters, F. S., and Bastiaens, P. I. (2001). Imaging FRET between spectrally similar GFP molecules in single cells. Nat. Biotechnol. *19*, 167–169.

Jakob, V., Schreiner, A., Tikkanen, R., and Starzinski-Powitz, A. (2006). Targeting of transmembrane protein shrew-1 to adherens junctions is controlled by cytoplasmic sorting motifs. Mol. Biol. Cell *17*, 3397–3408.

Kanekura, T., Chen, X., and Kanzaki, T. (2002). Basigin (CD147) is expressed on melanoma cells and induces tumor cell invasion by stimulating production of matrix metalloproteinases by fibroblasts. Int. J. Cancer *99*, 520–528.

Kataoka, H., DeCastro, R., Zucker, S., and Biswas, C. (1993). Tumor cell-derived collagenase-stimulatory factor increases expression of interstitial collagenase, stromelysin, and 72-kDa gelatinase. Cancer Res. *53*, 3154–3158.

Kirk, P., Wilson, M. C., Heddle, C., Brown, M. H., Barclay, A. N., and Halestrap, A. P. (2000). CD147 is tightly associated with lactate transporters MCT1 and MCT4 and facilitates their cell surface expression. EMBO J. *19*, 3896–3904.

Makuc, J., Cappellaro, C., and Boles, E. (2004). Co-expression of a mammalian accessory trafficking protein enables functional expression of the rat MCT1 monocarboxylate transporter in *Saccharomyces cerevisiae*. FEMS Yeast Res. *4*, 795–801.

McDonald, J. M., *et al*. (2006). The SHREW1 Gene, Frequently deleted in oligodendrogliomas, functions to inhibit cell adhesion and migration. Cancer Biol. Ther. *5*, 300–304.

Obrdlik, P., *et al*. (2004). K+ channel interactions detected by a genetic system optimized for systematic studies of membrane protein interactions. Proc. Natl. Acad. Sci. USA *101*, 12242–12247.

Osteen, K. G., Bruner, K. L., and Eisenberg, E. (1997). The disease endometriosis. In: Endometrium & Endometriosis, eds. M. P. Diamond and K. G. Osteen, Malden, MA: Blackwell Science.

Pushkarsky, T., Zybarth, G., Dubrovsky, L., Yurchenko, V., Tang, H., Guo, H., Toole, B., Sherry, B., and Bukrinsky, M. (2001). CD147 facilitates HIV-1 infection by interacting with virus-associated cyclophilin A. Proc. Natl. Acad. Sci. USA *98*, 6360–6365.

Rudiger, M., Jockusch, B. M., and Rothkegel, M. (1997). Epitope tag-antibody combination useful for the detection of protein expression in prokaryotic and eukaryotic cells. Biotechniques *23*, 96–97.

Saito, K., Oku, T., Ata, N., Miyashiro, H., Hattori, M., and Saiki, I. (1997). A modified and convenient method for assessing tumor cell invasion and migration and its application to screening for inhibitors. Biol. Pharm. Bull. *20*, 345–348.

Sameshima, T., Nabeshima, K., Toole, B. P., Yokogami, K., Okada, Y., Goya, T., Koono, M., and Wakisaka, S. (2000). Glioma cell extracellular matrix metalloproteinase inducer (EMMPRIN) (CD147) stimulates production of

membrane-type matrix metalloproteinases and activated gelatinase A in co-cultures with brain-derived fibroblasts. Cancer Lett. *157*, 177–184.

Starzinski-Powitz, A., Zeitvogel, A., Schreiner, A., and Baumann, R. (2001). In search of pathogenic mechanisms in endometriosis: the challenge for molecular cell biology. Curr. Mol. Med. *1*, 655–664.

Stein, G. S., Stein, J. L., Lian, J. B., Last, T. J., Owen, T. A., and McCabe, L. (1998). Synchronization of normal diploid and transformed mammalian cells. In: Cell Biology, A Laboratory Handbook, Vol. 1, ed. J. E. Celis, San Diego, London, Boston, New York, Sydney, Tokyo, Toronto: Academic Press, 253–258.

Sun, J., and Hemler, M. E. (2001). Regulation of MMP-1 and MMP-2 production through CD147/extracellular matrix metalloproteinase inducer interactions. Cancer Res. *61*, 2276–2281.

Toole, B. P. (2003). Emmprin (CD147), a cell surface regulator of matrix metalloproteinase production and function. Curr. Top Dev. Biol. *54*, 371–389.

White, P. S., *et al*. (2005). Definition and characterization of a region of 1p36.3 consistently deleted in neuroblastoma. Oncogene *24*, 2684–2694.

Wilson, M. C., Meredith, D., and Halestrap, A. P. (2002). Fluorescence resonance energy transfer studies on the interaction between the lactate transporter MCT1 and CD147 provide information on the topology and stoichiometry of the complex in situ. J. Biol. Chem. *277*, 3666–3672.

Zeitvogel, A., Baumann, R., and Starzinski-Powitz, A. (2001). Identification of an invasive, N-cadherin-expressing epithelial cell type in endometriosis using a new cell culture model. Am. J. Pathol. *159*, 1839–1852.

Zhou, S., Zhou, H., Walian, P. J., and Jap, B. K. (2005). CD147 is a regulatory subunit of the gamma-secretase complex in Alzheimer's disease amyloid beta-peptide production. Proc. Natl. Acad. Sci. USA *102*, 7499–7504.